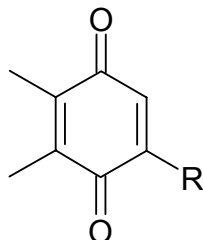# 5. Quinones in PSII

Instead of ubiquinone (Figure 3-0-1) in bRC from *Rb. sphaeroides*, PSII possesses plastoquinone (Figure 5-0-1) as electron acceptor, the primary (Q_A) and the secondary quinone (Q_B).

Figure 5-0-1. Plastoquinone. **R** stands for non-redox active part of aliphatic chain.

The ET from Q_A to Q_B in PSII is essential for photosynthesis. For instance, blocking this ET by herbicides (for instance, see DCMU in Figure 7-2-2 or DINOSEB in Figure 7-2-4), which bind in the Q_B binding pocket, stops photosynthesis, although it should be noted that the toxicity of these herbicides does not originate from the act of binding alone. The general view is that due to ET inhibition beyond Q_A the radical pairs generated by light enhance the possibility to form Chl*a* in the triplet state (reviewed in ref. (Rutherford and Krieger-Liszkay, 2001)).

Measurements of $E_m(Q_A)$ by redox titration indicated the existence of two PSII conformers with a difference of 145 mV in $E_m(Q_A)$, a low-potential Q_A form and a high-potential Q_A form (Krieger and Weis, 1992; Krieger et al., 1995). The high-potential form yields a larger E_m difference between Q_A and $Pheo_{D1}$ (see Figure 10-1-1) and favors a direct charge recombination of $P680^+Q_A^-$ (i.e. without involving the intermediate triplet generating $P680^+Pheo_{D1}^-$ state) (Johnson et al., 1995). Thus, the high-potential Q_A form has been proposed to play a photoprotective role in PSII. However, the mechanism of how PSII controls $E_m(Q_A)$ is still unknown. After its double reduction and protonation, Q_B is released from its binding site to the bulk quinone pool associated with the thylakoid membrane. Double protonation of Q_B to Q_BH_2 in PSII is considered to be an event analogous to that in bRC because of the high degree of structural similarity of the RC part in PSII and bRC (reviewed in refs. (Michel and Deisenhofer, 1988; Baymann et al., 2001; Rutherford and Faller, 2003)).

5.1. $E_m(Q_A)$ in PSII

The measured $E_m(Q_A)$ values are scattered in the range from –350 mV to +100 mV and can be assigned to three groups of –350 to –300 mV (lowest values), –100 to 0 mV (intermediate values) and +50 to +100 mV (highest values), as reviewed in ref. (Krieger et al., 1995). Low $E_m(Q_A)$ near –350 to –300 mV were found mainly in older studies (Cramer and Butler, 1969; Thielen and van Gorkom, 1981; Diner and Delosme, 1983) and the assignment of the measured potentials to $E_m(Q_A)$ may be a matter of debate (Rappaport et al., 2002).

We obtained $E_m(Q_A) = –148$ mV (Ishikita and Knapp, 2005e) in the 3.5 Å-structure (Ferreira et al., 2004), which can probably be assigned to the lower limit of the intermediate values of –100 mV. On the other hand, we obtained a much higher $E_m(Q_A)$ of –10 mV (Ishikita and Knapp, 2005e) in the 3.0 Å-structure (Loll et al., 2005). We did not interpret this value as belonging to the highest measured values of +50 to +100 mV, but rather attributed it to the lower limit 0 mV of the intermediate measured values. The

two crystal structures are identical in the H-bond pattern for Q_A, but in the 3.0 Å-structure H bonds to Q_A are stronger than those in the 3.5 Å-structure, which up-shifts the calculated $E_m(Q_A)$ for the former with respect to the latter. An interpretation of the highest measured $E_m(Q_A)$ of +50 to +100 mV is discussed later (for further details, see **10.1**).

5.1. Dependence of $E_m(Q_B)$ on H-bond pattern

5.1.1. H-bond flip of D1-Ser264

We found a remarkable change in H-bond pattern involving Q_B, D1-Ser264 and D1-His252, which depends not only on the redox state of $Q_B^{0/-}$ but also on the protonation state of D1-His252 (Ishikita and Knapp, 2005e). Hereby, the D1-Ser264 hydroxyl hydrogen forms an H bond with Q_B^0 (O – H distance 2.0 Å) in the presence of protonated D1-His252 (Figure 5-1-1b). Simultaneously, the D1-Ser264 hydroxyl oxygen is H-bonded with N_δ of D1-His252.

5.1.2. Calculated $E_m(Q_B)$

In response to the redox states Q_B^0 and Q_B^-, the geometry optimization procedure used in our computation yielded subtle variations in H-bond geometry involving the side chains of D1-His215, D1-Ser264 and the backbone amide group of D1-Phe265. These H-bond lengths varied by about 0.1 Å with the charge state of Q_B. The calculated $E_m(Q_B)$ yielded –95mV or –62 mV depending on whether the geometry optimization of hydrogen atoms was performed in presence of Q_B^0 or Q_B^-, respectively (Ishikita and Knapp, 2005e). Since $E_m(Q_B)$ is defined as a midpoint potential referring to an equal amount of Q_B^0 and Q_B^-, both conformations may be relevant. Consequently, we note that $E_m(Q_B)$ calculated in the presence of an H bond between Q_B and D1-Ser264 is in the range of –95 - –62 mV.

### 5.1.3. Driving force for ET from Q_A^- to Q_B

Together with the calculated $E_m(Q_A)$ of –148 mV, these two $E_m(Q_B)$ values provide an exergonic driving force of 53 meV and 86 meV for ET from Q_A to Q_B (Ishikita and Knapp, 2005e). From thermoluminescence studies, the free energy difference between Q_A and Q_B for one-electron reduction is estimated to be 70 meV (Robinson and Crofts, 1983), 80 meV (Crofts and Wraight, 1983) and 83meV (Minagawa et al., 1999) in agreement with our computational results.

If D1-His252 is in the charge neutral deprotonated state, the H bond of D1-Ser264 with Q_B^0 becomes weak and can be broken in the present study. Instead, the D1-Ser264 hydroxyl hydrogen is more likely to form an H bond with N_δ of D1-His252 (Figure 5-1-1a). In case of a reduced Q_B^-, however, the H bond of D1-Ser264 with Q_B exists regardless of the protonation state of D1-His252. The H bond between D1-Ser264 and Q_B^0 flip-flops with the D1-His252 protonation state and the formation of this H bond is favored if D1-His252 is protonated. The interplay of a permanent/fluctuating H bond between $Q_B^{-/0}$ and D1-Ser264 that is coupled to the D1-His252 protonation state could explain why Q_B^- is tightly bound to its binding site (de Wijn and van Gorkom, 2001) in contrast to the Q_B^0 in the neutral charge state.

Removing the H bond between D1-Ser264 and Q_B in PSII lowered the calculated $E_m(Q_B)$ dramatically from –95 - –62 mV in the presence of this H bond to –227 mV in its absence (Ishikita and Knapp, 2005e). A similar large down-shift of $E_m(Q_B)$ was also computed for bRC from *Rb. sphaeroides*, yielding –125 mV in the presence and –231 mV in the absence of the corresponding H bond (Ishikita and Knapp, 2004).

5.1.4. Similarity of Ser H-bond flip with bRC

Comparing PSII with bRC, the H-bond pattern at Q_B in PSII resembles the one in bRC from *Rb. sphaeroides*. In the latter, Q_B forms an H bond with the hydroxyl hydrogen of Ser-L223, depending on the protonation state of Asp-L213 (Alexov and Gunner, 1999; Ishikita and Knapp, 2004; Zhu and Gunner, 2005). According to the protein sequence alignment (analysis with CLUSTAL (Higgins et al., 1996)), Asp-L213 and Ser-L223 in bRC from *Rb. sphaeroides* correspond to D1-His252 and D1-Ser264 in PSII (Figure 5-1-1), implying a role of these residues in ET and protonation of Q_B.
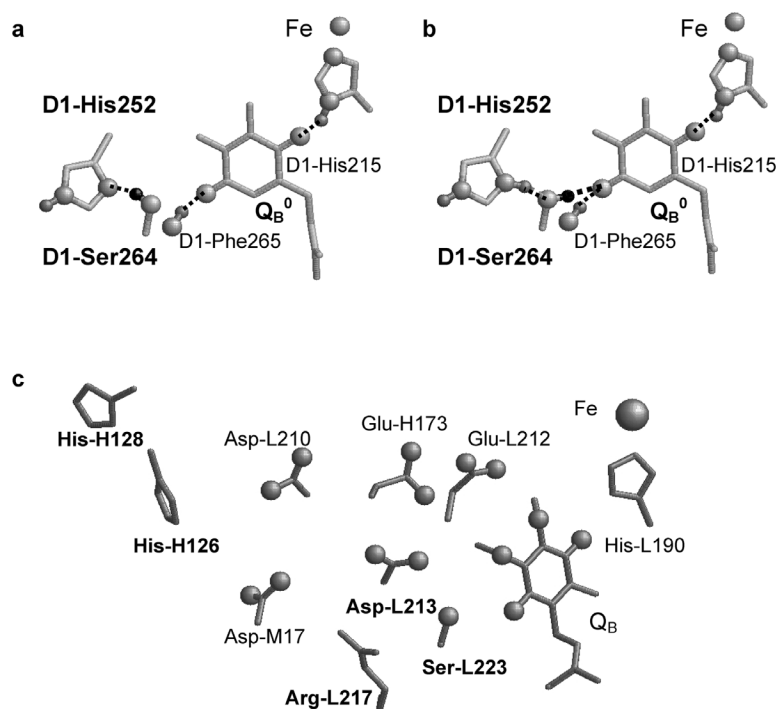
Figure 5-1-1. H-bond pattern at Q_B in PSII. **A)** for deprotonated D1-His252 and Q_B^0; **B)** for protonated D1-His252 and Q_B^0 or deprotonated D1-His252 and Q_B^-; **C)** residues in the proton transfer pathway of bRC from *Rb. sphaeroides* (Stowell et al., 1997).

5.2. Proton uptake at D1-His252 induced by the formation of Q_B^-

5.2.1. Absence of long PT pathways for Q_B in PSII

In bRC from *Rb. sphaeroides*, a cluster of several titratable residues in the neighborhood of Q_B, namely, His-H126, His-H128, Asp-M17, Asp-L210, Glu-L212, Asp-L213 and Ser-L223 was suggested to be involved in PT to Q_B, which is coupled to the ET from Q_A to Q_B (reviewed in ref. (Okamura et al., 2000), see Figures 4-2-1, 4-2-2 and 5-1-1b). In D1/D2 of PSII, there are no functionally equivalent titratable residues corresponding to His-H126, His-H128, Asp-L210 and Glu-L212 in bRC, while based on protein sequence alignment (analysis with CLUSTAL (Higgins et al., 1996)) Asp-L213 in bRC is replaced by D1-His252 in PSII (5-1-1a,b). Nevertheless, the existence of a proton transfer chain comparable to bRC was also suggested for PSII (Haumann and Junge, 1994). Indeed, recent kinetic studies in PSII revealed that ET from Q_A to Q_B is significantly slower in ^2H_2O than that in ^1H_2O (de Wijn et al., 2001), which strongly suggests the existence of a proton coupled ET reaction. The PSII crystal structure (Ferreira et al., 2004) supports the possibility that D1-His252 with its proximity to D1-Ser264 participates in protonation of Q_B.

5.2.2. Proton uptake at D1-His252

We found that, among all titratable residues in PSII, D1-His252 changes its protonation state most significantly in response to Q_B^- formation. With formation of Q_B^-, we observed a proton uptake of 0.56 H^+ at D1-His252 in the conformer with the H bond between Q_B and D1-Ser264 (Ishikita and Knapp, 2005e). Based on the PSII crystal structure, N_δ of D1-His252 can form a strong H bond with the hydroxyl oxygen of D1-Ser264 (N – O distance 2.5 Å), the latter forms simultaneously an H bond to the distal carbonyl oxygen of Q_B^- (O – O distance 2.8 Å). On the other hand, the corresponding proton uptake at D1-His252 is reduced to 0.15 H^+ only when D1-Ser264 reforms its H bond to D1-His252 instead to Q_B. Hence, it is likely that the formation of the H bond between Q_B and D1-Ser264 can extend the proton network from Q_B^- to D1-His252, forming a proton transfer channel from bulk solvent to Q_B^-. The corresponding Ser-L223 in bRC plays a crucial role for the ET from Q_A to Q_B and couples to proton uptake at Q_B (Paddock et al., 1995; Alexov and Gunner, 1999; Ishikita and Knapp, 2004; Paddock et al., 2005; Zhu and Gunner, 2005).

5.2.3. pK_a of D1-His252

In our computation, the pK_a of D1-His252 is 5.9 for Q_B^0 and increases to 7.3 for Q_B^- (Ishikita and Knapp, 2005e). Interestingly, Robinson and Crofts observed a titratable residue in thylakoid membranes whose pK_a shifts by about 1.5 units upon formation of Q_B^- (pK_a 6.4/7.9 for $Q_B^{0/-}$) (Robinson and Crofts, 1984). In a similar study, the Q_B^- state was stabilized at pH 7.6 (Vermaas et al., 1984), implying that ET from Q_A to Q_B is coupled with proton uptake at Q_B^- involving a titratable group at this pK_a. Since no other titratable residue showed such a large pK_a change upon formation of Q_B^- in the present study, we may assume that the titratable residue found in the two experimental studies is indeed D1-His252. If this is true, ET from Q_A to Q_B should be hampered by the interruption of this PT pathway.

5.2.4. Possible Cd^{2+} binding site at the acceptor side of PSII

Sigfridsson *et al.* (Sigfridsson et al., 2004) suggested that addition of Cd^{2+} to PSII hampers ET from Q_A to Q_B, without affecting Q_A redox-activity. Based on the PSII crystal structure (Ferreira et al., 2004), they proposed that the solvent exposed D1-His252 is involved in proton uptake at Q_B^- and a target of Cd^{2+} binding whose affinity to PSII is, however, relatively low (Figure 5-1-1a,b) (Sigfridsson et al., 2004). In bRC from *Rb. sphaeroides*, the Cd^{2+} binding site is formed by Asp-H124, His-H126 and His-H128 (Axelrod et al., 2000). This contrasts with PSII, which possesses no other titratable residues near D1-His252 since a protein corresponding to subunit H in bRC is lacking. This might explain the low affinity of PSII to bind Cd^{2+}. See also **4.2** for the Cd^{2+} binding site of bRC.

5.2.5. D1-Ser264 mutants

Our suggestion that D1-His252 and D1-Ser264 participate in the Q_B PT network is consistent with mutant studies, in which D1-Ser264 was replaced by Gly in PSII from two different species. In this mutant, it was observed that the rate of ET from Q_A to Q_B decreased in PSII from *Brassica napus* (Bowes et al., 1980) and the Q_B^- state was destabilized in PSII from *Synechocystis* PCC 6803 (Ohad and Hirschberg, 1992). The latter can be understood as a result of the removal of the H bond between Q_B and D1-Ser264. Therefore, we suggest that D1-His252 and D1-Ser264 are involved in proton transfer to Q_B. Proton uptake from the solvent occurs at D1-His252, while

D1-Ser264 transfers the proton to the distal carbonyl oxygen of Q_B. The decrease in rate of ET from Q_A to Q_B observed in ^2H_2O (de Wijn et al., 2001) may be related to proton uptake at D1-His252.

Conclusion:

Analog to the flip-flop H bond between Q_B and Ser-L223 in response to the protonation state of Asp-L213 in bRC, **we observed the corresponding H bond between Q_B and D1-Ser264 in response to the protonation state of D1-His252 in PSII. The consistence of the calculated pK_a of D1-His252** for the Q_B^0/Q_B^- redox states **to the experimentally observed pK_a** of an non-identified group in PSII suggests that **D1-His252 could play this role in the proton uptake event at Q_B**, and tha**t the H bond from D1-His252 is able to directly regulate the $E_m(Q_B)$ and the driving force of the forward ET from Q_A to Q_B.**